Journal of Engineering Physics and Thermophysics, Vol. 76, No. 3, 2003

AGGREGATION OF ERYTHROCYTES INTO COLUMNAR STRUCTURES ("ROULEAUX") AND THE RHEOLOGY OF BLOOD

L. A. Faitelson and E. E. Jakobsons

UDC 532.695:678-19

The liquid-crystalline order of the structure of blood, which is determined by the aggregation of erythrocytes into "rouleaux," i.e., liquid-crystalline domains, is considered. The form of the viscosity–rate of shear flow curve, specific for liquid-crystalline polymers, and the scaling regularities of the concentration dependence of the initial viscosity of erythrocyte suspensions are noted. An example of description and a prediction of the rheological functions of blood by the phenomenological model of an anisotropic viscoelastic liquid are given.

The development of modern hematology should be linked to the extraordinary powers of observation of the founder of scientific microscopy Leeuwenhoek (1632–1723), who in 1773, following Malpighi, discovered erythrocytes in blood and gave a detailed description of his investigations (1688). The next landmark in the study of blood was established by the results of investigations by the physiologist and physicist Poiseuille (1799–1869) of the resistance to the flow of viscous fluids in blood in thin tubes (1840). This was the beginning of hemorheology and of the application of its results to development of the mechanics of blood circulation.

The wide use of blood transfusion in medical practice and the development of hematology have resulted from Landsteiner's discovery of blood groups in the early 20th century (1901) [1, 2, p. 228].

At present, hemorheology has become a commonly recognized independent branch of biorheology. In 2002, the International Congress of Biorheologists and the IVth Conference on Clinical Hemorheology were held. The subjects of these scientific forums [3, p. 3] give an idea of the trends in modern biorheology and, in particular, hemorheology.

Introduction. Blood is a highly concentrated dispersion, mainly of red blood cells — erythrocytes (concentration of erythrocytes corresponds to the hematocrit Hct ≈ 45 vol.%) — and 1% of leucocytes and other blood cells in the plasma. It is assumed that the rheological properties of blood are determined mainly by the hematocrit and virtually do not depend on the presence of other blood cells. In the present report, we will adhere to the generally recognized viewpoint. However, at low deformation rates we might expect a manifestation of the effect of small additions [4] of other blood cells; this effect is well known in the rheology of polymers.

The shape of an erythrocyte at rest is a diskocyte (biconcave disk) whose diameter in the plasma is 8.4 μm, maximum thickness is ≈2.4 μm, minimum thickness is 1 μm, average volume is 87 μm^3, and surface area is 163 μm^2. The density of erythrocytes is 1.09 times higher than that of water. Among other blood cells, mention should be made of leucocytes, whose number is 10 to 20 times smaller than the number of erythrocytes, and thrombocytes, whose number is 10 times smaller than that of erythrocytes.

The viscosity of the fluid found inside an erythrocyte (mainly an almost saturated solution of hemoglobin) is 7 mPa·sec, which is approximately 5 times higher than the plasma viscosity (1.6 mPa·sec), which in turn is 1.6 times higher than the water viscosity. It follows that the viscosity of the contents of an erythrocyte exceeds approximately 7 times the viscosity of water (it has been indicated in [5, p. 39] that the plasma viscosity is 1.8 times higher than the water viscosity and this ratio is almost independent of the temperature and the rate of shear).

The shape of a biconcave disk, i.e., a diskocyte, determines the great flexibility of an erythrocyte, which manifests itself when blood is flowing in capillaries. It is remarkable that change in the erythrocyte shape occurs, according, for example, to [6], with preservation of constant volume and surface area by the erythrocyte. Hemolysis of erythrocytes occurs at a shear stress of about 200 Pa, at 10 Pa the cells are weakly deformed, and at 300 Pa the

Institute of Polymer Mechanics, Latvian University, Riga, Latvia; email: laf@edi.lv. Translated from Inzhenerno-Fizicheskii Zhurnal, Vol. 76, No. 3, pp. 214–225, May–June, 2003. Original article submitted January 27, 2003.

 1062-0125/03/7603-0728$25.00

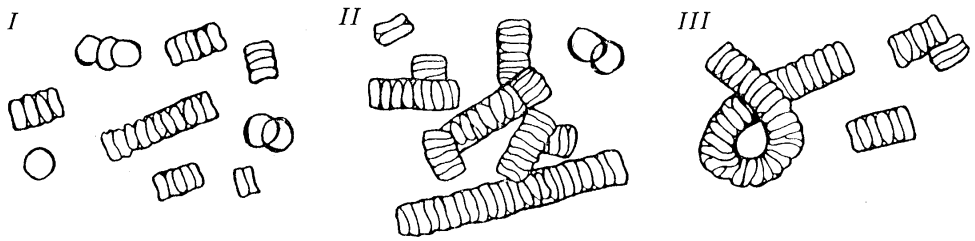

Fig. 1. "Rouleaux" of erythrocytes according to [8]: 1) rod-shaped short, II) rod-shaped long, and III) curved "rouleaux."

length of a deformed erythrocyte attains 30 μm. It has also been observed that a stress of 200 Pa is the absolute threshold below which there is no hemolysis (above 200 Pa, hemolysis depends on the duration of the action of stresses) [7, Chapter 10]. In what follows, we will adhere by convention to the highest value of the long axis of an extended ellipsoid (deformed erythrocyte) — 25 μm. The statement that the volume of an erythrocyte is constant, in practice, in its deformation is based on experimental data.

For the rheological properties of blood it is essential that aggregates — "rouleaux" of erythrocytes — are formed at rest and at low shear stresses (Fig. 1). The diameter of the "rouleaux" (of the erythrocytes in them) is larger than that of undeformed erythrocytes, while the thickness of the diskocytes is smaller. It can be inferred that attracting forces are acting between the erythrocytes in a rouleau. Apparently, "rouleaux" begin to form in the blood at values of the hematocrit higher than 12% and the blood viscosity acquires a dependence on the rate of shear [7, p. 182]. As the rate of shear increases, the length of the "rouleaux" decreases, and their disintegration occurs at a certain value of the shear stress. They twist (bend, become straightened) in the shear flow, which also, apparently, contributes to the viscosity decrease. However this cannot be the main and only reason for non-Newtonian viscosity, since the viscosity of an erythrocyte dispersion in the physiological salt solution in which "rouleaux" do not form also do not obey the Newtonian law of flow.

It is assumed that the deviations of the viscosity of an erythrocyte dispersion from the Newtonian viscosity are mainly determined by the deformation of the erythrocytes and their rotation in shear flows [7]. It is remarkable that an erythrocyte dispersion is capable of flowing even at Hct = 98%. We also note that about 3% of the plasma is "jammed" between the erythrocytes in "rouleaux" up to the destruction of the latter [9, p. 264]. An insight into the state-of-the-art of the practice and methods of clinical hemorheometry is given in [10, 11] and [12].

Erythrocytes. The cell membrane confining the cytoplasma of an erythrocyte consists mainly of lipid molecules forming a double layer with a thickness of about 75Å. The cytoplasma contains mainly hemoglobin, whose mass amounts to about 20% of the mass of blood. Only the "packing" of hemoglobin in discrete cells, i.e., erythrocytes, ensures the circulation of blood in the blood-vascular system. According to Pikin and Blinov [13], a fluid whose viscosity is equal to the viscosity of the cytoplasma could not perform its function in the body: only discrete cells with good hydrodynamic qualities enable the blood to easily penetrate into any region of the blood-vascular system. Below, we give data from the monograph of M. V. Vol'kenstein [14] which seem of importance for the rheology of blood (such ideas have also been presented in [15], p. 108]). The liquid-crystalline structure of the cell membrane (including the erythrocyte one) belongs to the class of A-type smectics [16, pp. 7 and 34] in which each layer is considered as a two-dimensional fluid. The smectic A phase is a laminar structure whose molecules inside the layers (in the direction perpendicular to the surface) act as fluids with oriented long molecular axes. The stability of shape for the liquid-crystalline erythrocyte membrane is provided by a spectrin-actin network very weakly attached to the membrane.

In shear blood flows, when the rates of shear are low, the "rouleaux" of erythrocytes and disaggregated erythrocytes perform "tumbles" during which the duration of rotational motion in the cycle is substantially shorter than the duration of flow in the position where the largest cross-sectional plane of an erythrocyte coincides with the plane of the Couette flow of the blood. Beginning with a certain rate of shear the erythrocyte ceases to "tumble" (beyond the aggregate); it is deformed in the flow and takes the shape of a triaxial ellipsoid (with axes $a \neq b \neq l$). This evolution of the erythrocyte shape in the flow has been noted even in [17, 18].

Geometry of an Erythrocyte and Erythrocyte Dispersions. According to the data of [19], the contour of the cross section of an erythrocyte is represented by a Cassinian oval (generalized lemniscate), and the erythrocyte shape is produced by the rotation of a Cassinian curve about the central axis (Fig. 2).

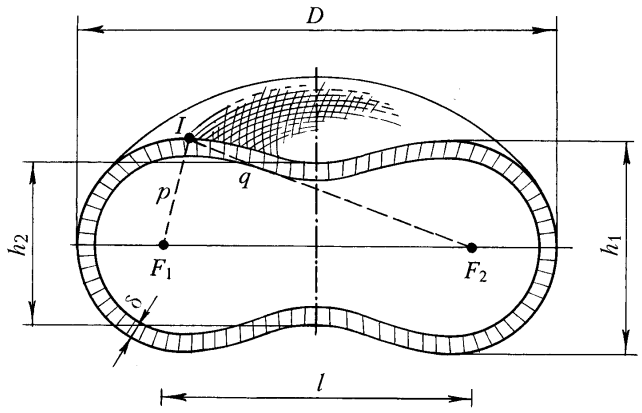

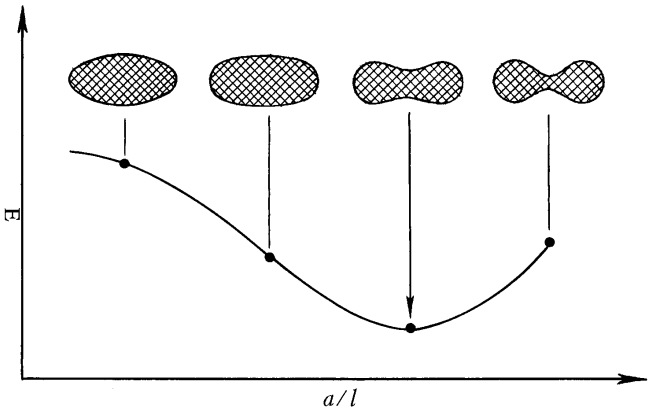

Fig. 2. Cassinian oval: l, distance between poles F_1 and F_2; p and q, distances from point I of the curve to poles F_1 and F_2.

Fig. 3. Deformation energy of the erythrocyte membrane E vs. a/l, i.e., shape factor of the Cassinian oval. The downward arrow shows the erythrocyte.

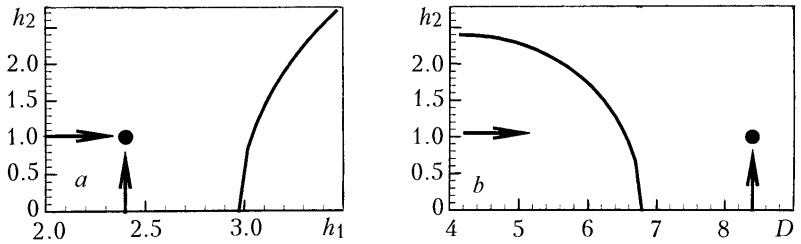

Fig. 4. Inapplicability of the equation of a Cassinian oval to the contour of the erythrocyte cross section: a) values of the erythrocyte thickness h_1 and h_2 satisfying the equation of a Cassinian oval for a diameter of the oval of D = 8.4 μm; b) values of the diameter and the thickness in the waist for the largest thickness h_1 = 2.4 μm. The arrows show the coordinates corresponding to the erythrocyte.

The shape of a Cassinian oval is substantiated by the fact that for the shape factor corresponding to the erythrocyte, i.e., for the ratio a/l, the deformation energy E of the highly elastic erythrocyte membrane passes through the minimum (Fig. 3). Furthermore, the shape of a Cassinian oval ensures rapid diffusion of oxygen into the erythrocyte hemoglobin [19]. We note that the membrane of the biconcave erythrocyte is the same throughout the length: dimples and convexities can occur on different portions of it (the pressure on the inside or the outside can be changed by ±15%) without causing wrinkling of the cell, i.e., there is a great lability in changing the cell shape "without accumulating elastic energy" [20, p. 41].

A Cassinian oval can be defined as the locus for which the product of the distances of two prescribed fixed points $F_1(l/2;\ 0)$ and $F_2(-l/2;\ 0)$ is a constant equal to a, i.e., $pq = a^2$. The equation of a Cassinian oval is $(x^2+y^2)^2 - 2c^2(x^2-y^2) - (a^4-c^4) = 0$. (In Fig. 2, we have introduced the notation $l = 2c$).

For $c < a < c\sqrt{2}$ the Cassinian oval is a closed line with a "waist." When $a > c\sqrt{2}$, the "waist" disappears and the curves take the shape of ellipse-like ovals.

Let us consider the suitability of a Cassinian curve for description of the outline of the erythrocyte cross section. We employ the generally recognized dimensions of an erythrocyte (in the plasma) [21].

Glaser's statement [19] that the contour of the erythrocyte membrane is described by a Cassinian oval is incorrect. In Fig. 4a, we plot the computed smallest thicknesse of an erythrocyte h_2 against its largest thickness h_1 on condition that the erythrocyte diameter is D = 8.4 μm. As is seen, the dimensions of the erythrocyte (h_1 = 2.4 μm and h_2 = 1.0 μm; they are shown on the coordinate axes as arrows) do not satisfy the equation of a Cassinian oval. The same is true of the dependence of h_2 on D — a diskocyte 8.4 μm in diameter with a constant largest thickness of the erythrocyte of h_1 = 2.4 μm cannot be described by a Cassinian oval.

TABLE 1. Influence of the Ratio of the Viscosities of the Droplet η and Dispersion-Medium η_m Fluids on the Ratio of the Periods of Circulation along the Streamline inside the Sphere T_v and on the Droplet Surface T_s

η_1/η_m	1.0	1.5	2.0	5.0	10	100
T_v/T_s	1.31	1.15	1.08	1.02	1.005	1.000

A number of other approaches to analytical description of the contour of the erythrocyte cross section are contained in [22] and [23, 24].

Critical Hematocrit Hct^*. The hematocrit Hct^* at which the packing of undeformed erythrocytes is the closest will be called critical (we disregard a certain increase in the diameter and decrease in the height of an erythrocyte in "rouleaux" [5]). For the above-mentioned geometric dimensions of an erythrocyte we have $Hct^* = V/V_c = 0.593$, where V_c is the limiting volume of a cell hexagonal in its cross section and with a height of $h_1 = 2.4$ μm into which the erythrocyte is inscribed. Thus, for the closest packing of undeformed erythrocytes we have $Hct^* = 59.3\%$.

Erythrocyte dispersions at $Hct > Hct^*$ must consist of predeformed and, apparently, prestressed erythrocytes. Since erythrocytes are never packed into parallel "rouleaux" (see Fig. 1), the value of the hematocrit $Hct_n \approx 40$–45% which is normal for healthy man probably corresponds to the maximum "random" packing of erythrocytes and, apparently, from purely theoretical considerations, we might expect two types of blood-flow curves: (a) $Hct < Hct_n$ and (b) $Hct \geq Hct_n$.

The erythrocyte not involved in "rouleaux" is rotating nonuniformly in the main at low rates of shear. However, beginning with a certain rate of shear it orients itself, its tumbling in the flow ceases, and the shape becomes ellipsoidal. At first, this is, apparently, a triaxial ellipsoid approaching an ellipsoid of revolution with increase in the shear stress. Let us consider precisely the latter scheme, assuming that, according to [7, p. 195], the erythrocyte can extend to 20–30 μm in the flow (until hemolysis occurs). Under deformation, the erythrocyte preserves constant volume ($V = 87$ μm^3) and surface area ($S = 163$ μm^2). We also assume that deformed erythrocytes (ellipsoids) have smectic order in the flow. In such a situation, the closest packing will be $Hct^{**} = 60.5\%$. This is somewhat higher than the ideal closest packing of undeformed erythrocytes $Hct^* = 59.3\%$. Whereas the long axis of an ellipsoid is $l = 20.5$ μm, its diameter (short axis) is $b = 2.85$ μm and $D/b = 8.4/2.85 = 2.94$. Consequently, the number of erythrocytes in the flow per unit cross section of the blood channel can change with the velocity of blood flow.

It is easy to determine the indices of a packing of deformed erythrocytes at other velocities of blood flow. Such rough estimates, with their obvious sketchiness, will be useful for clear representations related to hemorheology and many other processes of heat and mass exchange in the case of blood flow.

Other Approaches Explaining the Erythrocyte Shape. The laminar structure of the membrane, in the absence of liquid-crystalline order in the arrangement of molecules in the layer plane, is an indication of the liquid-crystalline (smectic) structure. The membrane layers — external and internal — have a somewhat differing molecular composition. These differences determine the dissimilar elasticities of the external and internal layers. Considering the energy expenditure in bending these layers, we are able to show that, for a certain pressure difference between the interior and the exterior of the cell membrane, it is more favorable for it to take a concave shape needed by the erythrocytes, since it contributes to their penetration into the capillaries and flow in them [13].

Blood: Emulsion of Erythrocytes in the Plasma. To compute the viscosity of diluted emulsions one usually employs the Taylor theory. If $1 > (\eta_1/\eta_m) > 0.5$, i.e., the viscosity of a droplet η_1 is lower than the viscosity of the matrix η_m, tangential stresses induce circulation flows along closed nearly elliptic trajectories inside the droplet. When the viscosity of the droplet is low ($\eta_1/\eta_m < 0.5$), two circulation flows occur near its center. In emulsions with a higher value of η_1/η_m, droplets orient themselves streamwise. Being initially spherical, they are extended before destruction with slow increase in the flow velocity — a neck forms. This is observed for all the employed values of the ratio of the droplet viscosities to the matrix viscosity on condition that the rate of shear increase very slowly (≈0.01 sec^{-1}/min) [25]. The periods of circulation of the fluid along the streamline of the sphere inside a spherical droplet T_v and on the sphere surface T_s are different (except for the case of a solid sphere where $T_v/T_s = 1$). Naturally, they are more than unity and depend on η_1/η_m. For the sake of comparison, Table 1 gives the calculated values borrowed from [26].

Addition of small amounts of surfactants to the formula of an emulsion, i.e., creation of an elastic shell around a droplet, leads to a cessation of the internal circulation in the droplet [25]. The results of observation of blood flow [17, 27] are seemingly inconsistent with the regularities established for emulsions of regular fluids. However, allowance should be made for the liquid-crystalline nature of the erythrocyte membrane. Whereas its viscosity can be compared to the viscosity of vegetable oil, according to the data of lateral diffusion [14], the viscosity in the direction transverse to the erythrocyte surface will be substantially lower. This is demonstrated by the twinkling of erythrocytes. The erythrocyte-membrane surface is a "soft medium" that changes its shape, i.e., it is subjected to local random deformations under the impacts ("impulses") of small molecules. These local and random deformations generate twinkling — each piece of the membrane surface acts as a rocking mirror. Twinkling, as de Gennes has established, is the "reflection" of molecular thermal motion [28]. Deformations in twinkling are predominantly realized in the normal direction to the surface of the membrane in which its viscosity is low.

Rolling of the Cytoplasma by the Membrane ("Tank-Tread Motion"). Studying the motion of two Heinz–Ehrlich bodies (employed as labels) one of which was found in the erythrocyte cytoplasma and the other of which was found on the membrane surface, Fischer and Schmidt-Schönbein have established that the membrane "rolls" the cytoplasma. They called this "rolling" "tank-tread motion" [17, 27]. Virtually linear dependences of the average angular rolling frequency ω_r on the rate of shear were noted in the cell deformed in the flow. These dependences are true for a viscosity of the continuous phase (the plasma was replaced by a dextran solution) of 18 to 140 mPa·sec. Shear flow of the continuum (matrix) is transferred to the cytoplasma in the form of circulation flows. In what follows, our interest will be with the erythrocyte taking the shape of triaxial ellipsoids in the flow. This occurs in normal blood (Hct = 40–45%) at the rates of shear $\dot{\gamma} \geq 500$ sec^{-1}; the long axes of the ellipsoids orient themselves in parallel to the direction of the flow. If a 5% suspension of erythrocytes is prepared from the same blood in the same plasma, there will be no orientation at the same rates of shear and deformed erythrocytes will rotate in the flow. If the plasma of blood was replaced by a dextran solution whose viscosity was severalfold higher than the plasma viscosity, we observed orientation of erythrocytes in the flow. It has been established that the elongation of erythrocytes is in proportion to the rate of shear.

In accordance with modern concepts, the shape of an erythrocyte is ensured by proteins that form the erythrocyte cytoskeleton. As follows from the model given in [29, p. 110] the flexible cytoskeleton allows rolling of the contents of the erythrocyte by the membrane and deformation of the erythrocyte (for penetration into capillaries). It is noted that rolling of the cytoplasma by the membrane contributes to a decrease in the blood viscosity.

For the suspension of erythrocytes in a dextran solution with a viscosity of 23 mPa it was established that $\omega_r = 0.03\dot{\gamma}$. The proportionality coefficient depended on the viscosity of the continuous phase [27].

Experimental Investigations of the Rheology of Blood. Hemorheology became a component part of hematology in the 1980s. The International Committee for Standardization in Hemorheology published a detailed report — "Guidelines for Measurement of Blood Viscosity and Erythrocyte Deformability" — reflecting the universally adopted methods of rheometry of blood [10]. Modern recommendations for hemorheological investigations are being worked out [11, 30]. The basic data obtained by 1980 on the rheological properties of blood are generalized in [5, 7, 31].

In [5, p. 49], there are, in particular, data of interest to us, namely: 1) blood is usually considered to be a non-Newtonian fluid and it, apparently, does not possess viscoelastic properties; 2) most of the available data on measuring the viscosity of blood can be described by the Casson equation for unidirectional flow; 3) all the attempts at detecting the action of normal stresses in shear flow of blood failed. Blood can be considered as a homogeneous fluid (at high rates of shear). Statements 1, 2, and 3 are essentially incorrect: the first of them was disproved by Lightfoot himself when he confined the applicability of the Casson model to the region of low (but not too close to the initial values of viscosity) rates of shear and to erythrocyte dispersions whose hematocrit does not exceed the normal values (to Hct $\approx$ 45%). In the region of high rates of shear (in artery flows), it is proposed that the rheological properties of blood be approximated by a Newtonian fluid. This assumption facilitates solution of the problems of circulatory dynamics and calculation of loads on circulatory assist devices but, apparently, it is insufficient in diagnostics (see, for example, [32]).

The statement that blood lacks viscoelasticity was disproved by the results given in [33]. Data on the viscoelasticity of blood are surveyed in the lectures of Quemada [31]. They give useful information on the reaction of blood mainly to the periodic shear at a frequency of 2 Hz with a successively (stepwise) increased amplitude of the defor-

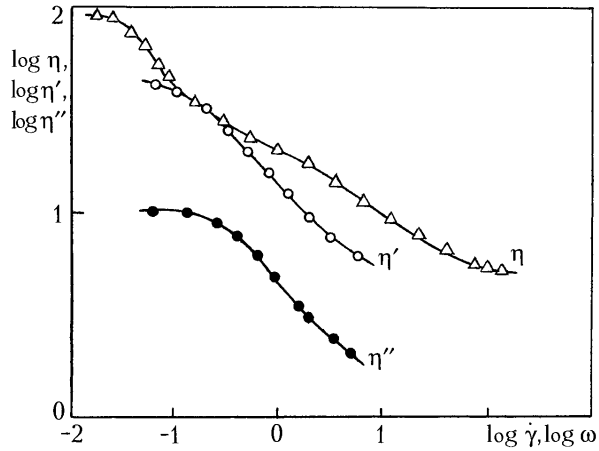

Fig. 5. Flow curve $\eta(\dot{\gamma})$ of normal blood (Hct = 45%) according to [38] and the frequency dependences of the linear viscoelastic functions, i.e., the real η' and imaginary η'' components of the complex viscosity of blood at Hct = 43% according to [3]. T = 22°C. η, η', and η'', mPa·sec.

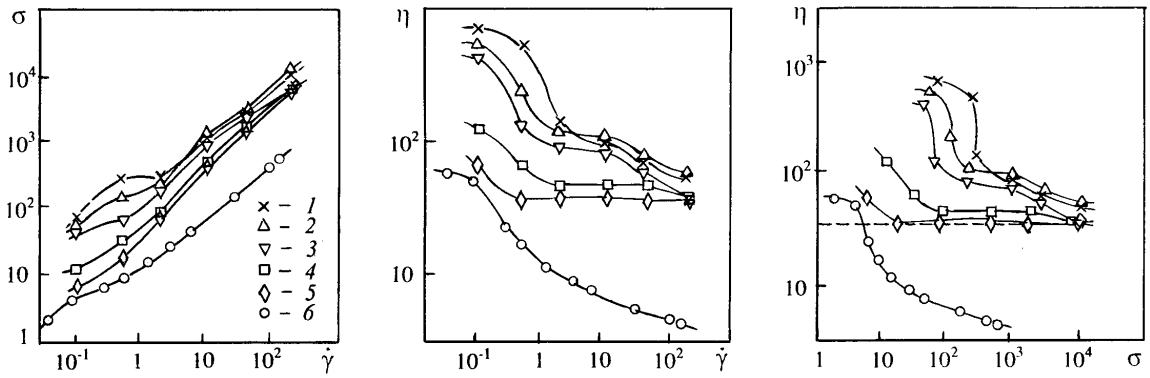

Fig. 6. Curves of flow of erythrocyte dispersions in dextran from the data of [17] for different levels of Hct (%): 1) 90; 2) 75; 3) 50; 4) 25; 5) 10 (T = 37°C); 6) the same of blood [39] for the hematocrit Hct = 39%. δ, mPa; η,

mation. The problem of large-amplitude periodic shear of nonlinear viscoelastic media, in particular, polymeric melts and solutions, has been studied by us in [34–36]. Naturally, we should proceed from small-amplitude frequency viscoelastic function, free of the typical nonlinear effects which are a function not only of the time of action but of its value as well. From [31], we reproduce in Fig. 5 the viscoelastic (frequency) functions $\eta'(\omega)$ and $\eta''(\omega)$ of normal blood (Hct = 45%) at a temperature of 22°C (the data of Chien [37]). In the same figure, we give the flow curve determined by Thruston [38] for normal blood at the same temperature but for Hct = 43%. The latter refer to another sample of "normal" blood. Nonetheless, to judge the expected values of the rheological characteristics we have resorted to the comparison mentioned. The effective viscosity η exceeds the values of the viscosity η' (and even the absolute value of the complex viscosity $|\eta^*|$) virtually throughout the investigated range of the rates of shear if we compare them at $\dot{\gamma} = \omega$. The imaginary component of the complex viscosity η'' in the same range of $\dot{\gamma}$ and ω is substantially smaller than the real component, i.e., $\tan\delta >> 1$.

The only investigation accessible to us in which both the function $\eta(\omega)$ and the functions $\eta'(\omega)$ and $\eta''(\omega)$ have been determined on the sample of one blood was Riha's publication [39], whose results are discussed in what follows.

Systematic investigation of the flow curves for different values of the hematocrit on dispersions which were prepared from heparinized-blood erythrocytes separated from the plasma by centrifuging with subsequent dilution of them in a 35% aqueous solution of dextran (M = 40,000) has been carried out by Schmid-Schönbein and Wells [17]. At 37°C, this solution had a constant viscosity independent of the rate of shear equal to 62 mPa·sec (erythrocytes do

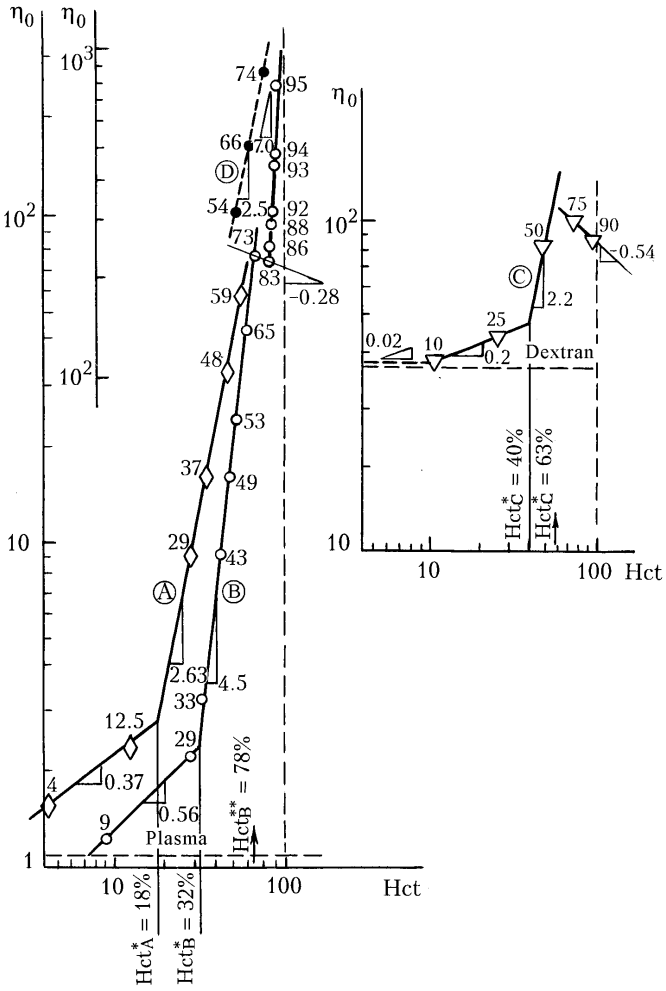

Fig. 7. Initial viscosity of erythrocyte dispersions in plasma vs. hematocrit (Hct, %): A) in plasma (with reduction to a temperature of 37°C) from the data of [43]; B) the same, at a temperature of 37°C from the data of [44]; C) of erythrocyte dispersions in a 35% aqueous solution of dextran at 37°C from the data of [17]; D) from the data of [52] at T = 25°C. Figures at the points, critical concentrations; slopes of the lines, scaling index; dashed lines, viscosity of the dispersion medium (plasma, dextran). η_0, mPa·sec.

not swell and do not shrink in a 35% aqueous solution of dextran). It is also known that in the dextran solution, unlike the physiological salt solution, erythrocytes are grouped into aggregates — "rouleaux." From the results obtained by these authors we constructed flow curves (Fig. 6). The character and shape of the dependences (particularly clearly $\eta(\sigma)$) varies in the range of values of the hematocrit from 25 to 50%. For Hct ≥ 50%, on attainment of certain critical values of σ^*, we have a "collapse", a sharp viscosity decrease caused, apparently, by the "disintegration of the structure." The hematocrit beginning with which the above transition is realized must be considered as critical Hct = Hct* (in the example in question, 25% < Hct* < 50%; probably, Hct* ≈ 40%). For the hematocrit Hct = 75% and at the rate of shear γ = 5 sec^{-1} we have "viscosity inversion," i.e., $\eta_{Hct_2} < \eta_{Hct_1}$ for $Hct_2 > Hct_1$. Such a phenomenon is characteristic of the solutions of liquid-crystalline polymers (decrease in the viscosity with increase in the concentration of a polymer). When Hct ≥ 50%, the flow curves correspond to the Onogi–Asada three- link scheme with portion II — "viscosity plateau" [40, p. 509]. Plotting the concentration dependence $\eta_0(c)$ for liquid-crystalline polymers, Papkov and Kulichikhin [41, 42] note that region I (at small $\dot{\gamma}$), according to the Onogi–Asada scheme, is a consequence of the uncontrolled disintegration of the supermolecular (domain) structure of a liquid-crystalline (LC) polymer. Therefore, according to Papkov and Kulichikhin, a theoretical rheology of LC polymers refers only to regions II and III of the

flow curve where the orientational situation is the same and there are no "declinations" and domains due to them. Indeed, constructing the concentration dependences $\eta_0(c)$ or $\eta_0(\mathrm{Hct})$, one should consider η on the viscosity "plateau" [42, p. 163]. But we attach much importance to portion I of the flow curve according to the Onogi–Asada scheme, particularly for description of the rheological properties of blood in which the erythrocytes form "rouleaux" the structure of which and the interaction between which are reflected precisely by region I of the flow curve. Therefore, we employ the rheological model capable of describing region I of the flow curve as well and of allowing for the polydomain liquid-crystalline state of the medium under study.

Dependence of the Initial Viscosity of Blood on the Hematocrit. Figure 7 (plot A) shows the dependence $\eta_0(\mathrm{Hct})$ constructed from the corrected data of Brooks et al. [43] obtained at a temperature of $T = 25^{\circ}\mathrm{C}$. The correction, i.e., temperature reduction, carried out in [44] lay in the fact that the ratio of the viscosities of plasma at 25 and $37^{\circ}\mathrm{C}$ for comparison was taken the same as the ratio of the viscosities of water at 25 and $37^{\circ}\mathrm{C}$. (Such temperature reduction invites separate study, despite the recommendations in [45], particularly for the region of low rates of shear.) The figures of the angles of slope of the straight lines reflect the scaling indices of the concentration dependence of the hematocrit. Transition from one type of connectivity to another [45–47] is realized for the values of the hematocrit Hct^* (arrows at the Hct axis). We also constructed such plots from the data of Zydney et al. [44] for the initial viscosity of the erythrocyte suspensions in plasma (B in Fig. 7) at $T = 37^{\circ}\mathrm{C}$. Curve C represents the data of Schmid-Schönbein and Wells for the erythrocyte dispersions in dextran [17] (we have employed the recommendations in [42, p. 163]). The logarithmic anamorphism enabled us to reveal scaling dependences and to establish a line of demarcation between the types of connectivity of the erythrocyte dispersions changing, as in polymeric solutions at critical concentrations [48–50]. Noteworthy are the portions of negative scaling indices for $\mathrm{Hct} > \mathrm{Hct}^*$ of the dispersions of series B and C characteristic of polymeric solutions transforming into the liquid-crystalline state (see, for example, [42, 46, 47; 51, pp. 430–433]). Figure 7, plot D, gives the concentration dependence of the initial viscosity of the dispersion of erythrocytes in plasma at $T = 25^{\circ}\mathrm{C}$ which has been determined from the data of [52]. The possibility of differentiating between the types of connectivity in liquid-crystalline polymeric solutions on the basis of a change in the scaling concentration dependence of the initial viscosity and compliance in shear was shown in [46]. There have been no data on the initial compliance in shear flows of blood as yet. Therefore, the results given in this section are to be refined by specially conducted experiments.

Limit Shear Stress σ_y. In monodisperse emulsions with a volume concentration of the dispersed phase higher than $c = 74$ vol.%, the spherical shape of droplets is disturbed and the concentrated emulsion becomes highly concentrated. Such emulsions are able not to spread — they acquire a comparatively easily determined yield stress σ_y. The stability of emulsions depends on the coefficient of surface interphase tension. In the case of erythrocyte–plasma this tension is extremely low, and the diskocyte shape is ensured by supercompliant intracellular bars consisting mainly of the structural protein spectrin. The limit shear stress of the blood of a healthy person is 1.5–5.0 mPa. To Hct = 42%, the value of σ_y linearly increases, but beginning with Hct = 42% it tends to saturation. Significant information on the limit shear stress of blood is contained in [52]. In this investigation, the regularities of $\sigma_y(\mathrm{Hct})$ are given. It also follows that from the flow curves, at particularly low rates of shear, one can directly evaluate the yield stress σ_y when working assemblies with a rough surface are employed. There is also the lower limit of hematocrit ($\mathrm{Hct} \approx 10\%$), below which the limit shear stress in blood is absent [7, p. 210]. In [11], σ_y is employed to compute the coefficient of cohesion of erythrocytes.

"Rouleaux" of Erythrocytes: "Liquid-Crystalline" Domains. In normal (healthy) blood, in the range of physiological temperatures the erythrocytes are grouped into aggregates, i.e., "rouleaux." The latter are analogs of liquid-crystalline domains, i.e., regions with the same orientation molecules. The size of the domains in liquid-crystalline polymers exceeds 10 μm [53], i.e., it is of the same order as the diameter of an erythrocyte and "rouleaux." The basic postulate of the rheometry of fluids — sticking of a fluid to boundary surfaces — is obviously legitimate under conditions where the units of flow are Brownian particles or supermolecular structures destroyed to the Brownian size by the shear flow.

From the data on measuring, at $25^{\circ}\mathrm{C}$, the flow curves shear stress–rate of shear of erythrocyte dispersions in plasma at the hematocrits Hct = 54, 66, and 74% covering rates of shear of 10^{-3} to 30 sec^{-1} [52], we have constructed the flow curves viscosity–shear stress (Fig. 8). We compared the flow curves measured in rheometers with smooth (polished) surfaces of the working assemblies and with rough surfaces. As is clear from the figure, when the

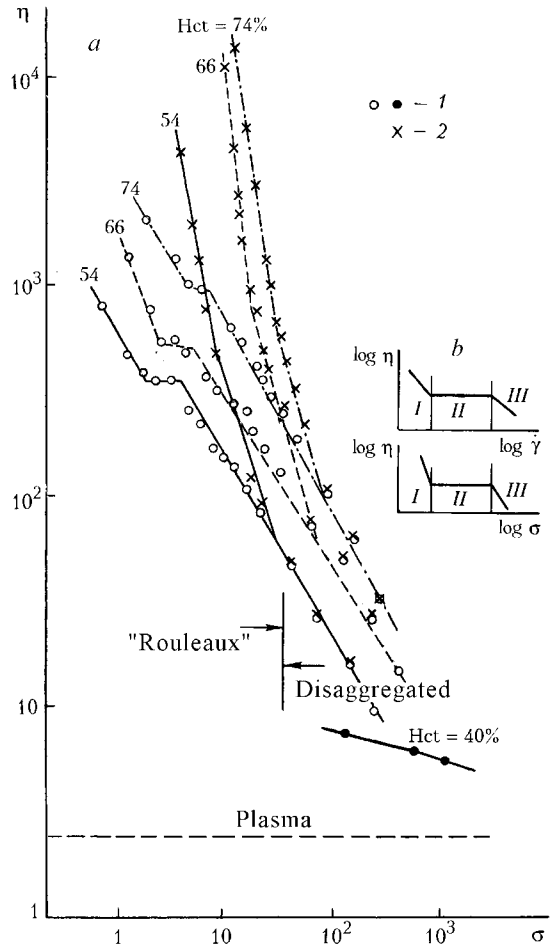

Fig. 8. Flow curves $\eta(\sigma)$ of blood at the hematocrit Hct = 54, 66, and 74% from the data of [52] and at Hct = 40% according to the measurements of M. G. Plyushch (a); diagrams of the flow curve of liquid-crystalline polymers according to Onogi and Asada [40] (6): 1) smooth surface and 2) rough surface. T = 25°C. η, mPa·sec; δ, mPa.

surfaces of the working assemblies are smooth, the flow curve of blood have three regions typical of liquid-crystalline polymers, including the region of the "viscosity plateau" (or *vice versa*, it may be assumed that the *I* region of the Onogi–Asada curve of flow of liquid-crystalline polymers (see the diagrams in Fig. 8b), too, is determined by the polydomain structure). We only note that in clinical rheometry the blood viscosity is usually determined in the range of the rates of shear of 20 to 200 sec^{-1} when the erythrocyte aggregates are already destroyed, in practice (see Fig. 8 for the data obtained by M. G. Plyushch at the A. N. Bakulev Scientific Center of Cardiovascular Surgery of the Russian Academy of Medical Sciences for Hct = 40%).

Blood shows thixotropy (see, for example, [31, p. 78)]. To be able to compare the characteristics of different samples of blood and to obtain measurement results free of poorly controlled structural changes in the process of preparation of the experiment one employs the preshear method [40, p. 414] in the rheometry of "combined media," in particular, emulsions. In [7, 11], beginning measurements for blood with such rates of shear above which disaggregation has obviously been completed, i.e., $\dot{\gamma} > 300$ sec^{-1}, are recommended and thereafter stepwise decreasing the prescribed rate of shear (in particular, recommended are rates of shear of 500, 300, 250, 150, 100, 75, 50, 25, 10, 5, and 1 sec^{-1}) with holding at each step until a practically steady-state shear stress is reached. The experiments described above, for example, [52], have been conducted precisely in order of a stepwise decreased rate of shear.

Rheological Phenomenological Model of an Anisotropic Viscoelastic Liquid and an Example of Determination of the Viscosimetric Functions of Blood. For analytical description of the rheological features of blood we

use the Akay–Leslie (A–L) phenomenological model of an anisotropic viscoelastic liquid [54]. The indicated model considers the liquid as a viscoelastic medium containing anisotropic or anisometric structural elements which orient themselves in flow. The rheological equation of state in a Cartesian coordinate system is prescribed in the form

$$\sigma_{ij} + \lambda \frac{D\sigma_{ij}}{Dt} = 2\eta_0 \dot{\gamma}_{ij} + (c_0 + c_1 \dot{\gamma}_{kr} n_k n_r)\, n_i n_j - 2c_2\, (\dot{\gamma}_{ik} n_k n_j + n_i n_k \dot{\gamma}_{kj})\,, \tag{1}$$

where the material parameters η_0 and λ have the dimensions of viscosity and time respectively, the influence of orientational effects is allowed for by the parameters of the model: c_0 having the dimensions of stress and c_1 and c_2 having the dimensions of viscosity, n_i are the components of the orientation vector or, what is the same, of the director, and $\dot{\gamma}_{ij} = \frac{1}{2}\left(\frac{dv_i}{dx_j} + \frac{dv_j}{fx_i}\right)$ is the deformation-rate tensor. The time derivative of the tensor field is prescribed in the form of the linear operator (introduced in [55])

$$\frac{DA_{ij}}{Dt} = \frac{dA_{ij}}{dt} + v_k \frac{dA_{ij}}{dx_k} - \omega_{ik} A_{kj} + A_{ik}\omega_{kj} + (1-\varepsilon)\, \dot{\gamma}_{ik} A_{kj} + (1-\varepsilon)\, A_{ik}\dot{\gamma}_{kj}\,, \tag{2}$$

where $\omega_{ij} = \frac{1}{2}\left(\frac{dv_i}{dx_j} - \frac{dv_j}{fx_i}\right)$ is the vortex (vorticity) tensor. As is seen, relation (1) is the equation of a Maxwell viscoelastic liquid that is generalized to finite deformations and to whose right-hand side there are added two terms allowing for the orientational effects of the medium's microstructure. If we set $\varepsilon = 1$ in (2), the operator is reduced to the Jaumann derivative of the tensor field with respect to time.

Microstructural orientation for the liquid in question is prescribed by the equation

$$\frac{Dn_i}{Dt} = d_0 n_k n_k n_i + \varepsilon_0 \dot{\gamma}_{ik} n_k + \varepsilon_1 \dot{\gamma}_{jk} n_j n_k n_i + f_0 \frac{D\dot{\gamma}_{ik}}{Dt} n_k + f_1 \frac{D\dot{\gamma}_{jk}}{Dt} n_j n_k n_i\,, \tag{3}$$

where the material parameters f_0 and f_1 related to the orientational vector (director) have the dimensions of time, d_0 has the dimension of frequency, and ε_0 and ε_1 are the dimensionless parameters. Orientation of the microstructure relative to the direction of flow is characterized by the modulus of the director and its direction. They depend in explicit form on the deformation rate.

We considered earlier the problems of steady-state shear flow and small-amplitude periodic deformation of the A–L liquid [56]. A comparison to experimental data for liquid-crystalline polymers and gels of microcrystalline cellulose [56, 57] showed a qualitative agreement, and it was inferred that the model must be modified for quantitative description of the measurement results, i.e., the spectrum of viscoelastic relaxation times must be taken into account.

The modification involved changing the expression for stresses (1) (with the orientation equation (3) being invariant).

We introduce the dimensionless parameters

$$C_0 = \frac{c_0 \lambda}{\eta}\,, \quad C_1 = \frac{c_1}{\eta}\,, \text{ and } \quad C_2 = \frac{c_2}{\eta} \tag{4}$$

into the equation of state. With account for (4), the equation of stresses (1) will be represented in the form

$$\sigma_{ij} + \lambda \frac{D\sigma_{ij}}{Dt} = 2\eta_0 \left[\dot{\gamma}_{ij} + \left(\frac{C_0}{\lambda} + C_1 \dot{\gamma}_{kr} n_k n_r\right) n_i n_j - 2C_2\, (\dot{\gamma}_{ik} n_k n_j + n_i n_k \dot{\gamma}_{kj})\right]. \tag{1′}$$

Then the viscosimetric function for the A–L model can be written as

$$\eta\,(\dot{\gamma}) = \frac{\eta_0}{2\,(1 + \lambda^2 \dot{\gamma}^2)} \left[2 + \left(\frac{C_0}{\lambda\dot{\gamma}} + C_1 n_1 n_2\right)(2n_1 n_2 + \lambda\dot{\gamma} n_2^2 - \lambda\dot{\gamma} n_1^2) - 2C_2\, |n|^2\right],$$

$$N_1(\dot\gamma) \equiv \sigma_{11} - \sigma_{22} = 2\lambda\dot\gamma\sigma_{12} + \eta_0\left(\frac{C_0}{\lambda} + C_1\dot\gamma n_1 n_2\right)(n_1^2 - n_2^2),$$
$$N_2(\dot\gamma) \equiv \sigma_{22} - \sigma_{33} = -\lambda\dot\gamma\sigma_{12} + \eta_0\left(\frac{C_0 n_2^2}{\lambda} + C_1\dot\gamma n_1 n_2^3 - 2C_2\dot\gamma n_1 n_2\right). \tag{5}$$

Here

$$|n| = \sqrt{\frac{f_0\dot\gamma^2(k^{-1}-k) - 2\varepsilon_0\dot\gamma}{2d_0(k^{-1}-k) + 2\varepsilon_1\dot\gamma - f_1\dot\gamma^2(k^{-1}-k)}}\ ,\quad n_1 = \frac{\mathbf{n}}{\sqrt{1+k^2}},\quad n_2 = \frac{1}{\sqrt{1+k^2}}\ \text{ and }\ k = \frac{f_0\dot\gamma + \sqrt{\varepsilon_0^2 - 1 + f_0^2\dot\gamma^2}}{\varepsilon_0 + 1}.$$

We will consider the small-amplitude periodic shear for the following two cases: 1) $d_0 = 0$ and consequently there is a certain initial anisotropy of the polydomain samples; 2) $d_0 < 0$, i.e., the sample is macroscopic.

The First Case ($d_0 = 0$). *The dynamic viscosity and the shear accumulation modulus.* The expressions for the components of the complex shear modulus are

$$\eta'(\omega) = \frac{\eta_0}{1+\lambda^2\omega^2}\left[1 + \frac{C_0(\varepsilon_0^2 f_1 - f_1 - \varepsilon_0\varepsilon_1 f_0 + \lambda\varepsilon_1)}{2\lambda\varepsilon_1^2} + \frac{C_1(\varepsilon_0^2 - 1)}{4\varepsilon_1^2} + \frac{C_2\varepsilon_0}{\varepsilon_1}\right],$$
$$G'(\omega) = \frac{\eta_0\lambda\omega^2}{1+\lambda^2\omega^2}\left[1 + \frac{C_0(\varepsilon_0^2 f_1 - f_1 - \varepsilon_0\varepsilon_1 f_0 + \lambda\varepsilon_1)}{2\lambda\varepsilon_1^2} + \frac{C_1(\varepsilon_0^2 - 1)}{4\varepsilon_1^2} + \frac{C_2\varepsilon_0}{\varepsilon_1}\right]. \tag{6}$$

The Second Case ($d_0 < 0$). Since, as has been shown in [4], the vector of the initial orientation in this case is $\mathbf{n}_0 = 0$, all the combinations of the director components and their derivatives with respect to time are equal to zero and the reaction to periodic shear by small amplitudes will be the same as the reaction of a Maxwell isotropic linear viscoelastic liquid.

In modifying the A–L model, we introduce the discrete spectrum of viscoelastic-relaxation times and additionally the asymptotic viscosity η_∞. Then the governing equation (1′) can be written in the form

$$\sigma_{ij} = \eta_\infty\dot\gamma_{ij} + \sum_{p=1}^{N}\sigma_{ij(p)}, \tag{7}$$

$$\sigma_{ij(p)} + \lambda_p\frac{D\sigma_{ij(p)}}{Dt} = \eta_p\left[2\dot\gamma_{ij} + \left(\frac{C_{0(p)}}{\lambda_p} + C_{1(p)}\dot\gamma_{kr}n_k n_r\right)n_i n_j - 2C_{2(p)}(\dot\gamma_{ik}n_k n_j + n_i n_k\dot\gamma_{kj})\right],$$

where $C_{0(p)}$, $C_{1(p)}$, and $C_{2(p)}$ are the dimensionless parameters:

$$C_{0(p)} = \frac{c_0\lambda_p}{\eta_p},\quad C_{1(p)} = \frac{c_1}{\eta_p},\quad \text{and}\quad C_{2(p)} = \frac{c_2}{\eta_p}. \tag{8}$$

The material functions for the modified model follow from Eqs. (7) and (8) with account for (5) and (6).

The Steady-State Shear Flow ($\dot\gamma$ = const):

$$\eta(\dot\gamma) = \sum_{p=1}^{N}\frac{\eta_p}{2(1+\lambda_p^2\dot\gamma^2)}\left[2 + \left(\frac{C_{0(p)}}{\lambda_p\dot\gamma} + C_{1(p)}n_1 n_2\right)(2n_1 n_2 + \lambda_p\dot\gamma n_2^2 - \lambda_p\dot\gamma m n_1^2) - 2C_{2(p)}n^2\right] + \eta_\infty,$$

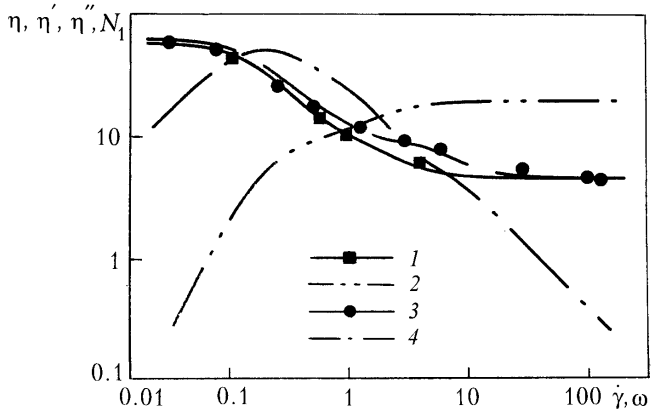

Fig. 9. Shear viscosity η (1) and first difference of normal stresses N_1 (2) vs. rate of shear $\dot{\gamma}$ and material η' (3) and imaginary η'' (4) components of the complex viscosity vs. deformation frequency for blood ω containing a citrate solution as an anticoagulant (hematocrit Hct = 39%). Points, experimental results according to [39], curves, calculation from the modified A–L model. T = 37°C. η, η', and η'', mPa·sec.

$$N_1(\dot{\gamma}) \equiv \sigma_{11} - \sigma_{22} = \sum_{p=1}^{N} \left[2\lambda_p \dot{\gamma} \sigma_{12(p)} + \eta_p \left(\frac{C_{0(p)}}{\lambda_p} + C_{1(p)} \dot{\gamma} n_1 n_2 \right) (n_1^2 - n_2^2) \right], \tag{9}$$

$$N_2(\dot{\gamma}) \equiv \sigma_{22} - \sigma_{33} = \sum_{p=1}^{N} \left[-\lambda_p \sigma_{12(p)} + \eta_p \left(\frac{C_{0(p)} n_2^2}{\lambda_p} + C_{1(p)} \dot{\gamma} n_1 n_2^2 - 2C_{2(p)} \dot{\gamma} n_1 n_2 \right) \right].$$

The Small-Amplitude Periodic Shear ($\dot{\gamma}(t) = \gamma_0 \omega \cos \omega t$):

$$\eta'(\omega) = \eta_\infty + \sum_{p=1}^{N} \frac{\eta_p}{1 + \lambda_p^2 \omega^2} \left[1 + \frac{C_{0(p)} (\varepsilon_0^2 f_1 - f_1 - \varepsilon_0 \varepsilon_1 f_0 + \lambda_p \varepsilon_1)}{2\lambda_p \varepsilon_1^2} + \frac{C_{1(p)} (\varepsilon_0^2 - 1)}{4\varepsilon_1^2} + \frac{C_{2(p)} \varepsilon_0}{\varepsilon_1} \right], \tag{10}$$

$$G'(\omega) = \sum_{p=1}^{N} \frac{\eta_p \lambda_p \omega^2}{1 + \lambda_p^2 \omega^2} \left[1 + \frac{C_{0(p)} (\varepsilon_0^2 f_1 - f_1 - \varepsilon_0 \varepsilon_1 f_0 + \lambda_p \varepsilon_1)}{2\lambda_p \varepsilon_1^2} + \frac{C_{1(p)} (\varepsilon_0^2 - 1)}{4\varepsilon_1^2} + \frac{C_{2(p)} \varepsilon_0}{\varepsilon_1} \right].$$

To find the material constants and parameters of the model in the general case we must simultaneously approximate experimental data on both the steady-state shear flow and the periodic shear, as follows from dependences (9) and (10).

On the models of viscoelastic liquids, the requirement that the viscous and elastic characteristics of a material be described in both the linear and nonlinear regions of flow is imposed. However, despite the great body of data published on hemorheology, we were able to find only one reference [39] in which the results of measurements in both the linear and nonlinear regions of deformation are given. To describe these data using the modified A–L model we employed the discrete spectrum given in the mentioned publication. We determined the parameters of the model, minimizing the sum of the squares of the relative derivatives of the calculated data from the experimental data for both $\eta(\dot{\gamma})$ and $\eta'(\omega)$ simultaneously. The results are shown in Fig. 9, and the found values of the parameters are given in Table 2.

It follows from the figure that we are able to quantitatively describe the experimental data by the modified model. The figure also represents the predicted dependence of the first difference of normal stresses on the rate of

Table 2. Parameters of the Modified Model of Akay and Leslie for the Blood Sample [39]

c_0, mPa	c_1, mPa·sec	c_2, mPa·sec	d_0, $\sec^{-1}$	ε_0	ε_1	f_0, sec	f_1, sec
5.4	–262	–19	–11.5	3.9	–5.1	–1.61	1.61

shear. The calculation shows that the values of N_1 are less than 30 mPa in the investigated range, which is much lower than the sensitivity of the rheometers manufactured at present. This result explains the absence of data on the $N_1(\dot{\gamma})$ of blood and lends impetus to a search for methods assisting one in measuring the nonlinear elastic properties of blood. Knowledge of these properties will enable one to investigate the stability of the medium's structures occurring in shear flows [58].

CONCLUSIONS

The liquid-crystalline order of erythrocytes belongs to the columnar nematic structure of diskocyte objects, i.e., erythrocytes whose aggregates forming "rouleaux" are an analog of liquid-crystalline domains. The destruction of these domains by a shear flow leads to the viscosity–rate-of-shear-flow curve characteristic of liquid-crystalline polymers and consisting of three portions. The scaling regularity of the dependence of the initial viscosity of blood on the hematocrit has been revealed. The applicability of the modified phenomenological rheological model of Akay and Leslie to description of the rheology of blood and prediction of its elastic properties has been shown.

This work was carried out with financial support from the Latvian Council on Science.

NOTATION

$\mathrm{Hct_n}$, normal hematocrit; Hct^*, critical hematocrit (change in the scaling index); Hct^{**}, hematocrit beginning with which the sign of the scaling index changes; D, h_1, and h_2, diameter and the largest and smallest thicknesses of an erythrocyte, m; V, erythrocyte volume, m^3; S, surface area of an erythrocyte, $\mu\mathrm{m}^2$; T, temperature, $^{\circ}\mathrm{C}$; M, molecular mass; T_v, periods of circulation along the streamline in the spherical-drop volume, sec; T_s, periods of circulation along the streamline on the spherical-drop surface, sec; a, b, and $l = 2c$, parameters of the Cassinian oval and the ellipsoid axis ($l > b > a$), m; k, tangent of the angle of direction of the orientation vector; c_0, c_1, and c_2, parameters of the Akay–Leslie model, Pa·sec, Pa, and Pa; C_0, C_1, and C_2, dimensionless parameters of the Akay–Leslie model; $C_{0(p)}$, $C_{1(p)}$, and $C_{2(p)}$, dimensionless parameters of the modified Akay–Leslie model; t, running time; d_0, parameter of the equation of microstructural orientation, $\sec^{-1}$; f_0 and f_1, parameters of the orientation vector, sec; n_i, components of the orientation vector; $\mathbf{n}$, orientation vector; $\mathbf{n}_0$, vector of the initial orientation; $|n|$, modulus of the orientation vector; N_1 and N_2, first and second differences of normal stresses, Pa; G', shear modulus of accumulation, Pa; η_0, initial viscosity, material parameter, Pa·sec; η, effective shear viscosity, Pa·sec; η_∞, asymptotic viscosity, Pa·sec; η' and η'', real and imaginary components of the complex shear viscosity, Pa·sec; η_1, viscosity of the dispersed phase of the emulsion, Pa·sec; η_m, viscosity of the dispersion medium (matrix) of the emulsion, Pa·sec; $\dot{\gamma}$, rate of shear, $\sec^{-1}$; $\dot{\gamma}_{ij}$, deformation-rate tensor, $\sec^{-1}$; ω, angular frequency, $\sec^{-1}$; ω_r, average angular frequency of rolling of the membrane cytoplasma, $\sec^{-1}$; ω_{ij}, vortex tensor, $\sec^{-1}$; σ_{ij}, stress tensor, Pa; σ_y, limit shear stress (yield stress), Pa; λ, material parameter, sec; ε, ε_0, and ε_1, dimensionless parameters of the equation of microstructural orientation; δ, thickness of the erythrocyte membrane, m. Subscripts: n, normal; v, volume; s, surface; m, matrix; r, rotation; c, critical.

REFERENCES

1. B. Seeman, *The River of Life. The Story of Human Blood from Magic to Science*, New York (1961).
2. J. Folta and L. Nový, *Dejiny prirodnych vied v datach*, Bratislava (1981).
3. Proceedings XI Int. Congr. of Biorheologists and IX Int Conf. on Hemorheology, *Tromboz Gemostaz Reologiya*, No. 2, 3 (2002).
4. Yu. S. Lipatov, in: *Book of Abstracts of Papers and Reports presented at XII Mendeleev Congr. on General and Applied Chemistry* [in Russian], No. 2, Moscow (1981), pp. 179–180.

5. E. N. Lightfoot, *Transport Phenomena and Living Systems*, New York (1974).
6. E. I. Shafranova and N. S. Snegireva, *Mekh. Kompozit. Mater.*, **5**, No. 4, 42–50 (1999).
7. C. G. Caro, T. J. Pedley, R. C. Schroter, and W. A. Seed, *The Mechanics of the Circulation*, Oxford–New York (1978).
8. I. Ya. Ashkinazi, *Erythrocyte and Internal Thromboplastin Formation* [in Russian], Leningrad (1977).
9. G. I. Kozinets and V. A. Makarov, *Study of the Blood System in Clinical Practice* [in Russian], Moscow (1997).
10. International Committee for Standardization in Hematology (Expert Panel on Blood Rheology). Guidelines for Measurement of Blood Viscosity and Erythrocyte Deformability. *Clinical Hemorheol.*, No. 5, 439–453 (1986).
11. E. V. Roitman, N. N. Firsov, M. G. Dement'eva, N. N. Samsonova, M. G. Plyushch, and N. A. Vorob'eva, *Tromboz Gemostaz Reologiya*, No. 3, 5–12 (2000).
12. E. V. Roitman, N. N. Firsov, M. G. Dement'eva, N. N. Samsonova, M. G. Plyushch, and N. A. Vorob'eva, in: *Problems of the Rheology of Polymers and Biomedicinal Systems* [in Russian], Interinstitutional Collection of Scientific Papers, Saratov (2001), pp. 97–104.
13. S. A. Pikin and L. M. Blinov, *Liquid Crystals* [in Russian], Moscow (1982).
14. M. V. Volkenshtein, *General Biophysics* [in Russian], Moscow (1978).
15. A. Rees and M. Sternberg, *From Cells to Atoms*, Oxford (1984).
16. P.-G. de Gennes, *The Physics of Liquid Crystals*, Oxford (1974).
17. H. Schmid-Schönbein and R. Wells, *Science*, **165**, No. 3890, 288–291 (1969).
18. S. D. Zakharov, *Fiz. Zhivogo* (*Nov. Zhizni Nauka Tekhnika*), *Ser. Fiz.*, No. 10, 41–63, Moscow (1985).
19. R. Glaser, *Biologie einmal anders*, Leipzig (1974).
20. G. I. Kozinets, *Interpretation of Blood and Urine Analyses and Their Clinical Importance* [in Russian], Moscow (1998).
21. A. I. Vorob'ev and Yu. I. Lorie (eds.), *Manual on Hematology* [in Russian], Moscow (1979).
22. E. A. Evans and R. Skalak, *Mechanics and Thermodynamics of Biomembranes*, Florida (1980).
23. B. S. Bull and J. D. Brailsford, *Blood*, **41**, No. 6, 833–844 (1973).
24. H. J. Deuling and W. Helfrich, *Biophys. J.*, Vol. 16, 861–868 (1976).
25. V. N. Kuleznev, *Polymer Mixtures* [in Russian], Moscow (1980).
26. P. Sherman, in: P. Sherman (ed.), *Emulsion Science* [Russian translation], Leningrad (1972), pp. 197–312.
27. T. M. Fischer and H. Schmid-Schönbein, *Blood Cells*, **3**, 351–365 (1977).
28. P.-G. de Gennes and J. Badoz, *Les Objects Fragiles* [Russian translation], Moscow (2000).
29. *Wintrobe's Clinical Hematology*, 9th edn., Vols. 1 and 2, Philadelphia–London (1993).
30. International Committee for Standardization in Hematology. Recommendation for a Selected Method for the Measurement of Plasma Viscosity, *J. Clinical Pathol.*, **37**, 1447–1452 (1984).
31. D. Quemada, in: C. M. Rodkiewicz (ed.), *Arteries and Arterial Blood Flow*, Courses and Lectures No. 270. Int. Centre for Mechanical Sciences. Wien (1983).
32. M. M. Tanashyan, V. G. Ionova, M. A. Karabasova, L. V. Motova, and E. G. Demina, *Tromboz Gemostaz Reologiya*, No. 3 (11), 42–45 (2002).
33. A. L. Copley, R. G. King, S. Chien, S. Usami, R. Skalak, and C.-R. Hung, *Biorheology*, **12**, 257–263 (1975).
34. L. A. Faitelson, *Dokl. Akad. Nauk Latv. SSR*, No. 3, 42–49 (1965).
35. L. A. Faitelson and M. G. Tsiprin, *Mekh. Polim.*, No. 3, 515–522 (1968).
36. I. P. Briedis, Yu. T. Yakovlev, and L. A. Faitelson, *Mekh. Polim.*, No. 3, 428–437 (1968).
37. S. Chien, in: N. H. C. Hwang, D. R. Gross, and D. J. Patel (eds.), *Quantitative Cardiovascular Studies*, Baltimore (1979), pp. 241–287.
38. G. B. Thruston, *Biorheology*, **16**, 149–162 (1979).
39. P. Řiha, *Rheologica Acta*, **21**, No. 4/5, 650–652 (1982).
40. R. G. Larson, *The Structure and Rheology of Complex Fluids*, New York–Oxford (1999).
41. V. S. Kulichikhin, V. S. Matveev, V. I. Yankov, M. D. Gluz, and V. G. Kulichikhin. *The Obtaining and Properties of Solutions and Melts of Polymers* [in Russian], Moscow (1994).
42. S. P. Papkov and V. G. Kulichikhin, *Liquid-Crystalline State of Polymers* [in Russian], Moscow (1977).

43. D. E. Brooks, J. W. Goodwin, and G. V. Seaman, *J. Appl. Physiol.*, **28**, 172–177 (1970).
44. A. L. Zydney, J. D. Oliver, and C. K. Colton, *J. Rheol.*, **35**, No. 8, 1639–1704 (1991).
45. J. Harkness, in: J. D. O. Lowe, J. C. Barbenal, and C. D. Fobers (eds.), *Clinical Aspects of Blood Viscosity and Cell Deformability*, New York (1981), p. 79.
46. E. Jakobsons and L. A. Faitelson, in: I. Emri and R. Cvelber (eds.), *Progress and Trends in Rheology. Proc. Fifth Eur. Rheology Conf.*, Darmstadt (1998), pp. 232–233.
47. G. Kiss and R. S. Porter, in: W. Brostow (ed.), *Mechanical and Thermophysical Properties of Polymer Liquid Crystals*, London (1998), pp. 343–406.
48. L. Z. Rogovina and G. L. Slonimskii, *Vysokomolek. Soed. B*, **39**, No. 6, 1543–1556 (1997).
49. A. N. Semenov and M. Rubinstein, *Macromolecules*, **31** 1373–1397 (1998).
50. J. E. Martin, D. Adolf, and J. P. Wilcoxon, *Physiol. Rev. A*, **39**, No. 3, 1325–1332 (1989).
51. M. Doi and S. F. Edwards, *The Theory of Polymer Dynamics* [Russian translation], Moscow (1998).
52. C. Picart, J.-M. Piau, and H. Calliard, *J. Rheol.*, **42**, No. 1, 1–12 (1998).
53. H. Wang, M. C. Newstein, M. Y. Chang, N. R. Balsara, and B. A. Garetz, *Macromolecules*, **33**, 3719–3730 (2000).
54. G. Akay and F. M. Leslie, in: B. Mena, A. Garcia-Rejo, and C. Rangel-Nafaile (eds.), *Advances in Rheology*, Vol. 3, Mexico (1984), pp. 495–502.
55. A. E. Everrage and R. J. Gordon, *J. Appl. Polym. Sci.*, **7**, 317–328 (1974).
56. E. Yakobson and L. A. Faitel'son, *Mekh. Kompozit. Mater.*, **33**, No. 6, 821–839 (1997).
57. E. Jakobsons, L. Faitelson, and M. Laka, in: H. Münstedt, J. Kaschta, A. Merten (eds.), *Proc. 6th Eur. Conf. on Rheology*, Erlangen (2002), pp. 83, 84.
58. E. Jakobsons and L. Faitelson, in: *Proc. XIIIth Int. Congr. on Rheology*, Cambridge, 2000, Vol. 3 (2000), pp. 116–118.